Institute of Physics Publishing Nanotechnology
Nanotechnology **16** (2005) 2764–2769 doi:10.1088/0957-4484/16/12/003

# Formation and *in situ* dynamics of metallic nanoblisters in $Ga^+$ implanted GaN nanowires

**A Datta[1,6], S Dhara[1,7], S Muto[2], C W Hsu[3], C T Wu[3], C H Shen[3], T Tanabe[2], T Maruyama[4], K H Chen[1,3], L C Chen[3] and Y L Wang[1,5]**

[1] Institute of Atomic and Molecular Sciences, Academia Sinica, Taipei 106, Taiwan
[2] Department of Nuclear Engineering, Graduate School of Engineering, Nagoya University, Nagoya 464-8603, Japan
[3] Center for Condensed Matter Sciences, National Taiwan University, Taipei 106, Taiwan
[4] The Wakasawan Energy Research Center, 64-52-1, Hase, Tsuruga 914-0192, Japan
[5] Department of Physics, National Taiwan University, Taipei 106, Taiwan

Received 3 June 2005, in final form 22 August 2005
Published 11 October 2005
Online at stacks.iop.org/Nano/16/2764

**Abstract**
The formation of voids and bubbles in the energetic ion implantation process is an important issue in material science research, involving swelling induced embrittlement of materials in nuclear reactors, catalytic activities in the nanopores of the bubble, etc. We report here the formation and *in situ* dynamics of metallic nanoblisters in GaN nanowires under self-ion implantation using a $Ga^+$ focused ion beam. High-resolution transmission electron microscopes equipped with electron energy loss spectroscopy and energy filtering are used to identify the constituents of the blister. *In situ* monitoring, with focused ion beam imaging, revealed the translation and rotation dynamics of the blisters.

## 1. Introduction

Voids and bubbles are formed as a consequence of displacement damage and injection of inert gases or disintegration and simultaneous accumulation of gaseous component of target material [1–4], during ion beam interaction with materials beyond the fluence of amorphization. The formation of a three-dimensional (3D) void-lattice has demonstrated the earliest example of self-organization [5] in material processing which is the key concept of 'bottom-up' technology for modern-day ultra-small-scale device formation. Understanding of void or bubble formation addressed issues of swelling and embrittlement in detecting material failure in modern technology, e.g. materials used for nuclear reactors. Smart cut technology, to produce high quality silicon on insulator (SOI) wafers in industrial scale, is also a manifestation of defects produced by the accumulation of gases in the implantation process [6]. At the same time, buried damage layers, created by high energy ion implantation far from the active device area of a semiconductor, have been shown to provide efficient proximity gettering centres for impurity metals and micro-defects far from the electrical junction region [7]. Recently, bubble formation in a Cu matrix has found applications as catalyst [8]. The formation of voids and bubbles leading to volume swelling in metal or alloys [9] seems to have a similar influence in both elemental and compound semiconductors [3, 4, 10]. This is a common feature in two-dimensional (2D) film and 3D bulk systems with less pronounced defect mobility than that in a 1D nanowire (NW) system. For subsurface implantation profile, as in the case of low energy implantation, surface deformation in the form of blistering is reduced or eliminated [9, 11]. The mobility of the gaseous species is shown to be greatly enhanced with the reduction of localized accumulation of gaseous species for the growth of blisters or bubbles.

The present study is related to the formation of metallic nanoblisters in $Ga^+$ implanted GaN NWs and its *in situ* dynamics. GaN NWs grown on a c-Si wafer are implanted with a 50 keV focused ion beam (FIB) of $Ga^+$ for various fluences. Field emission scanning electron microscopy (FESEM) is used to observe the nanoblisters *ex situ*. High-resolution transmission electron microscopy (HRTEM) imaging along

[6] Now at: Amity Institute of Nanotechnology, Amity University, Noida-201 303, UP, India.
[7] Author to whom any correspondence should be addressed. The author is on leave from: Materials Science Division, Indira Gandhi Centre for Atomic Research, Kalpakkam-603 102, India.

with energy filter imaging assisted with electron energy loss spectroscopy (EELS) are performed for the identification of the true constituent of the nanoblisters. The imaging facility of the FIB is used for simultaneous implantation and *in situ* monitoring of the nanoblister dynamics, after the nanowires are brought very close to the fluence for nanoblister formation.

## 2. Experimental details

Randomly oriented GaN NWs were formed by a chemical vapour deposition technique using molten gallium as the source and 10 sccm $NH_3$ as reactant gas. Thin film Au (∼5 nm) was used as the catalyst in the vapour–liquid–solid growth mechanism of GaN NWs. The NWs formed are in the wurtzite phase. Details of the sample preparation, morphological studies and structural identification are published elsewhere [12–15].

Using FIB, these nanowires were irradiated with 50 keV $Ga^+$ self-ion to a fluence of $2 \times 10^{20}$ m$^{-2}$. The FIB was raster scanned over an area of 400 $\mu$m × 400 $\mu$m with a beam current of ∼1.3 nA corresponding to an ion flux of $\sim 5 \times 10^{16}$ ion m$^{-2}$ s$^{-1}$ ($\sim 15.6 \times 10^{-3}$ dpa s$^{-1}$), which is comparable to the reported [4] value for irradiation studies in the epitaxial (epi-) GaN film. It is followed by nominal number scans in a small area of 4 $\mu$m × 4 $\mu$m for further irradiation and simultaneous observation of nanoblister formation with an ion flux $1 \times 10^{17}$ ions m$^{-2}$ s$^{-1}$ with a very small beam current of 1.1 pA. A Monte Carlo based SRIM code [16] calculation shows that the 50 keV $Ga^+$ in GaN is a nuclear energy loss (∼2 keV nm$^{-1}$) dominated process with a projected range of ∼24 nm. Compared to a broad ion beam, FIB is preferred for the implantation process as it is more mono-energetic (energy spread <0.2%) [17], leading to a better defined longitudinal straggling of the collision cascades created by the ions in the 1D NW.

## 3. Results and discussion

Figure 1 shows typical FESEM (Jeol-JSM-6700F) and TEM (Jeol-JEM4000EX) images of the nanoblisters (50–200 nm) formed by 50 keV $Ga^+$ self-ion implantation on GaN NWs. The fluence used was of $2 \times 10^{20}$ ions m$^{-2}$, corresponding to a damage of ∼62 displacements per atom (dpa), as calculated from the simulated defect analysis data using SRIM code [16].

For identification of the nanoblister (figure 2(a)), EELS (Gatan digiPEELS model 766, attached to a Jeol-JEM200CX TEM; probe size 10 nm, energy resolution 1.5 eV) spectra in the plasmon-loss region corresponding to blister and NW regions (figure 2(b)) show the presence of pure Ga (13.6 eV) and GaN (19.6 eV) [18], respectively. Nitrogen K-edge spectra (figure 2(c)) for the NW region correspond to results typical for GaN [19]. A small hump at 19.6 eV in the plasmon spectrum corresponding to the blister region (figure 2(b)) results from the very thin layer of amorphous GaN (a-GaN) supporting the nanoblister (amorphous nature shown in figure 2(d)).

HRTEM imaging (figure 3) with a 1 MV electron source (Hitachi H-1250ST) was used for structural study for the blister region. Lattice imaging of the blister on the top shows a crystalline lattice corresponding to Ga. The lattice corresponds to GaN in the NW region. An FFT power spectrum (to avoid the problem of not getting a good crystalline selected area electron diffraction pattern corresponding to Ga lattice, as the localized temperature of the probe area might melt Ga (melting point ∼302.8 K)) was calculated for the corresponding lattice images. The zone axes correspond to $[01\bar{1}]$ and [110] for $\alpha$-Ga and wurtzite-GaN phases, respectively (figure 3(b)). Ga is a metallic molecular crystal with $Ga_2$-dimer as the building block for the FCC orthorhombic $\alpha$-Ga phase [20]. Moreover, the Ga–Ga distance in the GaN lattice is the same as in metallic Ga owing to the small radius of the N atom [21]. So, Ga atoms around nitrogen vacancies ($V_N$s) form strong metallic bonds during the disintegration process. Large energy deposition during the 50 keV self-ion ($Ga^+$) implantation in GaN nanowires also favours the formation of $V_N$s, as the formation energy of a single $V_N$ is only 4 eV in GaN [22]. Thus, the nucleation of the $\alpha$-Ga phase is quite likely during the chemically clean self-ion implantation process with a large possibility of creation of $V_N$s during the disintegration process generating a large number of $Ga_2$-dimers as building blocks. In our previous report, we have also discussed the stability of the crystalline $\alpha$-Ga phase by calculating pressure inside a typical blister [11]. The broadened Bragg spots corresponding to the GaN lattice (figure 3(b)) may arise from the disordering and mosaic (small domains slightly misaligned to each other) nature of the crystalline GaN that occurred upon irradiation. These defects may be correlated mainly to the large-scale vacancies of Ga, which might have been disintegrated from GaN.

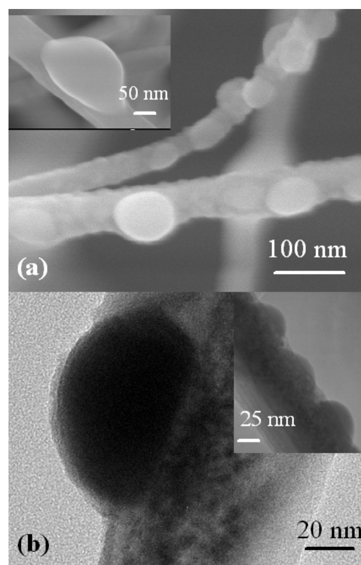


**Figure 1.** Microscopic images of the nanoblisters formed at 50 keV $Ga^+$ implantation on GaN nanowires with a fluence of $2 \times 10^{20}$ ions m$^{-2}$. (a) FESEM images of the nanoblisters (diameter ∼50–100 nm). The inset shows a large nanoblister (diameter ∼200 nm). (b) TEM of a nanoblister (diameter ∼100 nm). The inset shows an array of nanoblisters (diameters ∼75 nm).

Energy filter (Jeol JEM3000F transmission electron microscope equipped with Gatan Imaging Filter) images of the nanoblister formed at 50 keV $Ga^+$ implantation on GaN nanowires with a fluence of $2 \times 10^{20}$ ions m$^{-2}$ are shown in figures 4(a)–(d). The bright field TEM image is seen in figure 4(a) for the nanoblister (dark region with possible

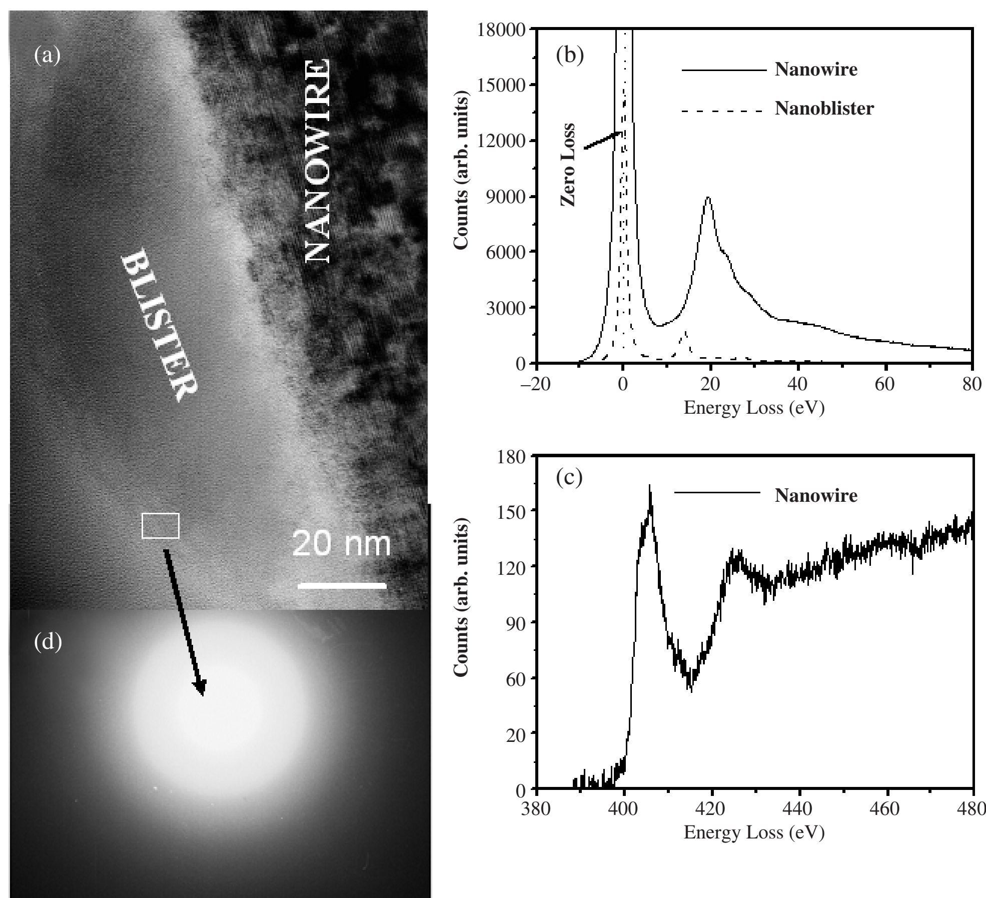


**Figure 2.** EELS in the plasmon-loss region. (a) HRTEM image of nanoblister formed at 50 keV $Ga^+$ implantation on GaN nanowires with a fluence of $2 \times 10^{20}$ ions $m^{-2}$ shown to guide the regions studied. (b) Plasmon-loss spectra corresponding to the nanoblister and nanowire region. (c) N K-edge spectrum corresponding to the nanowire region. (d) Selected area electron diffraction pattern corresponding to the amorphous layer supporting the nanoblister.

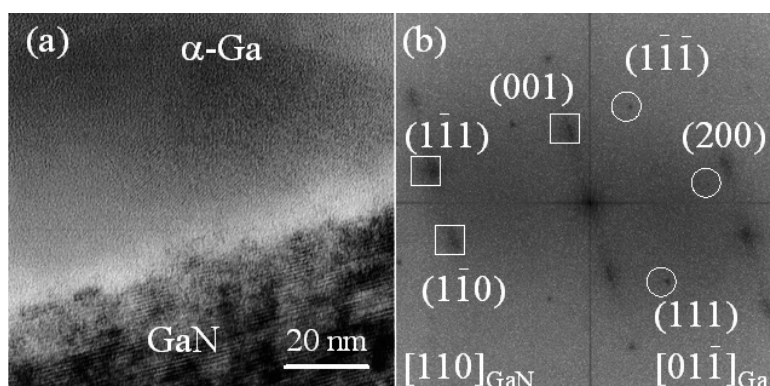


**Figure 3.** HRTEM imaging with a 1 MV electron source. (a) Lattice imaging of nanoblisters (top) formed at 50 keV $Ga^+$ implantation on GaN nanowires with a fluence of $2 \times 10^{20}$ ions $m^{-2}$ in the $\alpha$-Ga phase and nanowire (underneath) wurtzite-GaN phase. (b) Calculated FFT power spectrum corresponding to the lattice images. The zone axes correspond to $[01\bar{1}]$ and [110] for $\alpha$-Ga and wurtzite-GaN phases, respectively.

high electron density) and adjacent nanowire region. The thickness distribution image in figure 4(b) shows a pattern formed at the image plane of the objective lens containing information about mass-thickness distribution through the illuminated area of the sample. Elemental mapping also showed Ga deficiency (figure 4(c)) in the nanowire region adjacent to the blister. Nitrogen deficiency (figure 4(d)) in the blistered region confirmed Ga as the main constituent. The contribution of Ga from the ion source falling in the base area of the blistered region is calculated to be only ~4.0 nm. The major amount of Ga contributing to the blister formation may be from the adjacent lattice, which shows disordered or mosaic

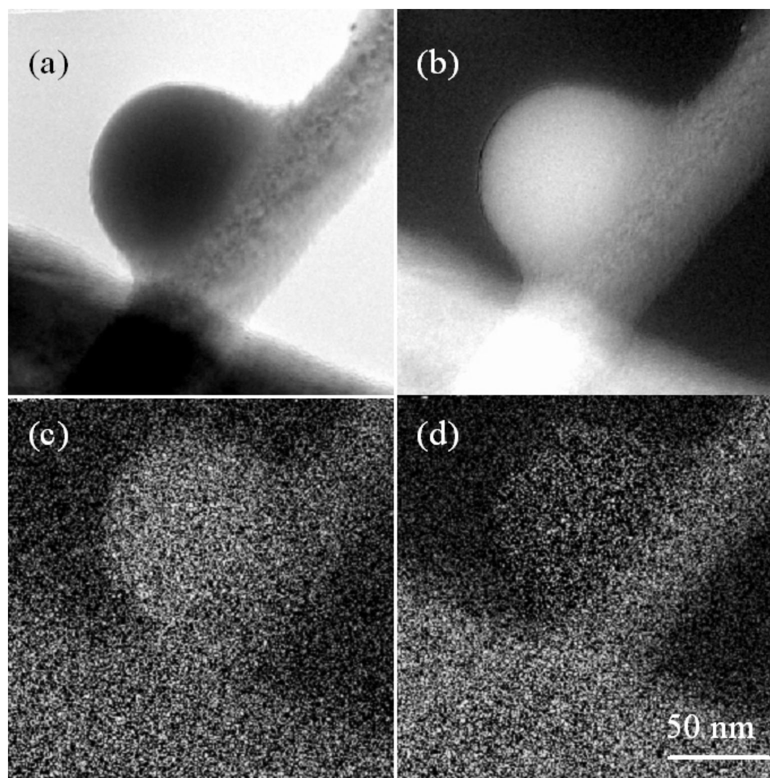


**Figure 4.** Energy filter (Jeol JEM3000F transmission electron microscope equipped with Gatan Imaging Filter) images of the nanoblister formed at 50 keV $Ga^+$ implantation on GaN nanowires with a fluence of $2 \times 10^{20}$ ions $m^{-2}$. (a) Elastic (bright field TEM) image, (b) thickness distribution image (see text for details), (c) Ga elemental mapping, (d) N elemental mapping.

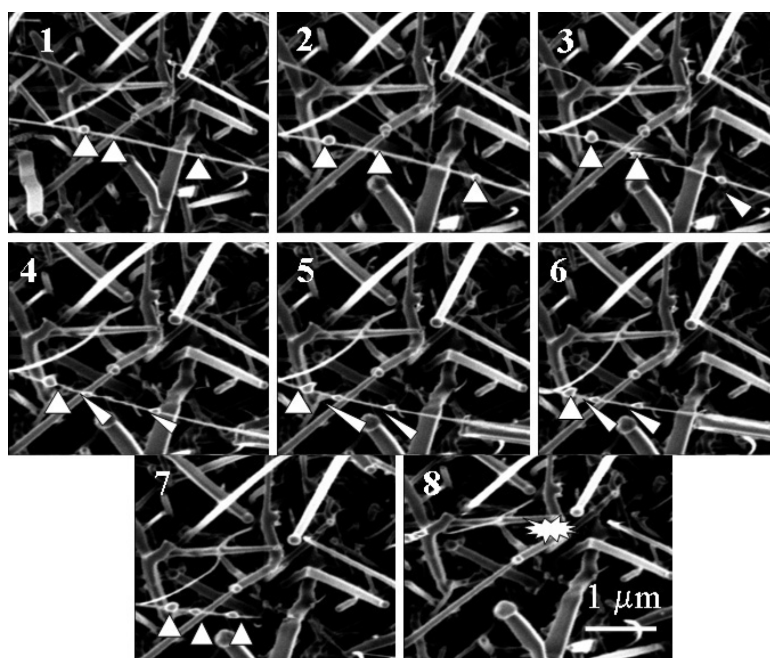


**Figure 5.** Focused ion beam (FIB) imaging for the *in situ* growth, translation dynamics and final rupture of the nanoblisters with sequential $Ga^+$ rastering. Translational motions are indicated with arrows.

nature in lattice spacing (figure 3(a)) owing to probable Ga vacancy-related defects. Radiation-enhanced diffusion (RED) of either $Ga^+$ or the lattice disintegrated Ga from a sufficiently large distance in the NW and contribution to the accumulation process also cannot be ruled out in this heavy-ion implantation process containing large cascades. The formation of gaseous

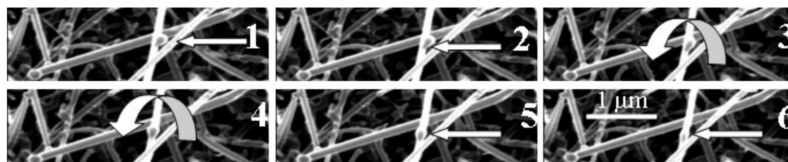


**Figure 6.** Focused ion beam (FIB) imaging for the *in situ* growth and rotational dynamics of a single nanoblister. The blister and rotational motion are indicated with arrows.

bubbles with the accumulation of nitrogen disintegrated from the GaN lattice in the energetic process is suppressed with the low-energy implantation process. The higher mobility of gaseous species at subsurface implantation with low-energy FIB (range ∼24 nm as calculated from SRIM code [16]) impedes localized accumulation for further growth of gaseous bubbles [9, 11].

Interestingly, we also observed the *in situ* dynamics of these nanoblisters during a progressive ion implantation process. The FIB imaging facility was used to observe the motion of these nanoblisters, taking an image after each rastering process. We first located an arbitrary region of the sample containing GaN NWs on a c-Si substrate and irradiated up to $2 \times 10^{20}$ ions $m^{-2}$, keeping the identical irradiation conditions, as described for the formation of blisters, in an area of 400 $\mu$m × 400 $\mu$m. After almost reaching the fluence of $2 \times 10^{20}$ ions $m^{-2}$ we chose an area of 4 $\mu$m × 4 $\mu$m within the irradiated 400 $\mu$m × 400 $\mu$m box and started irradiating with an increased amount of flux $\sim 1 \times 10^{17}$ ions $m^{-2}$ $s^{-1}$ in order to record the observable dynamics. The first image was taken in the 4 $\mu$m × 4 $\mu$m, and then with progressive rastering of the $Ga^+$ beam we could monitor the growth as well as the movement of the nanoblisters and sometimes the rupture of the nanoblisters. The translational motion is shown in figure 5, frame-by-frame. We took the first image and found that typically three nanoblisters were observed on a GaN NW. Then with progressive rastering of the ion beam we registered both the growth as well as the movement of the nanoblisters towards each other; finally the blisters ruptured after a sufficient amount of rastering. Similarly, in a different location we focused our attention on a rotating (counterclockwise) nanoblister with progressive fluence (figure 6). Though we could not find any exact experimental evidences for the mechanism for these dynamic events, the following comments may be stated with our common understanding and small amount of evidence found during the study. The movement is probably assisted by the accumulation of gaseous nitrogen and simultaneous tendency for this to get released thorough defected regions inside the NW, guiding the precipitates to grow and move. The first movement of accumulated gas breaking the stiff GaN (the bulk modulus being very high in GaN: ∼210 GPa [23]) wall inside the NW might generate a shock wave, as was observed in one of the frames (third frame in figure 5). Sometimes during the implantation process at high fluences the accumulated nitrogen gas could also get released out of the NW through the defected area and a surface pore was observed (figure 7) near the blister region imparting a rotation (figure 6) to the blister. Rapture of the nanoblister occurs when the supporting a-GaN (figures 2(a), (d)) layer fails to hold the accumulated precipitates.

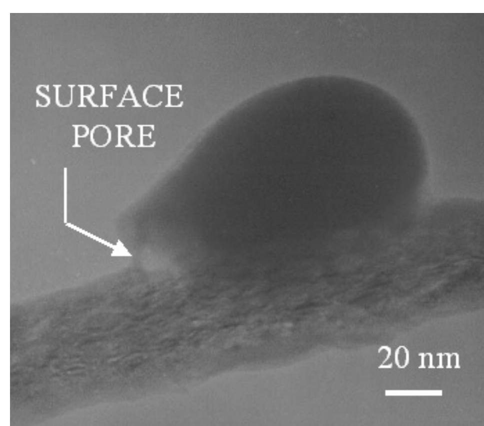


**Figure 7.** TEM (Jeol JEM-4000EX) image of the pore near the blister indicating a possible pathway for the release of accumulated nitrogen gas.

## 4. Conclusions

Thus the nanoblisters originate with the agglomeration of heavier element (Ga) in the subsurface implantation process at low energy. The accumulated Ga is found in the crystalline phase, which may have nucleated with the formation of $Ga_2$-dimer (in the absence of nitrogen) as the building block for the FCC orthorhombic $\alpha$-Ga phase. The translational and rotational dynamics of the nanoblisters are proposed to be guided by the movement of accumulated gaseous nitrogen during the disintegration process.

## Acknowledgments

The authors would like to acknowledge the National Science Council (NSC), Taiwan for financial support in pursuing this study. We also acknowledge K G M Nair, MSD, IGCAR, Kalpakkam, India for useful discussions during the preparation of the manuscript.

## References

[1] Wiffen F W 1971 *Radiation-Induced Voids in Metals* ed J W Corbett and L C Lanniello (New York: Albany) pp 386–96
[2] Johnson P B 1991 *Fundamental Aspects of Inert Gases in Solids* ed J H Evan and S E Donnelly (New York: Plenum) p 167
[3] Kucheyev S O, Williams J S, Jagadish C, Zou J, Craig V S and Li G 2000 *Appl. Phys. Lett.* **77** 1455
[4] Kucheyev S O, Williams J S, Zou J, Jagadish C and Li G 2000 *Appl. Phys. Lett.* **77** 3577
[5] Krishnan K 1980 *Nature* **287** 420
[6] Celler G K and Cristoloveanu S 2003 *J. Appl. Phys.* **93** 4955

[7] Wong H, Cheung N W, Chu P K, Liu J and Mayer J W 1998 *Appl. Phys. Lett.* **52** 1023
[8] Gilberd P W, Johnson P B, Vickridge I C and Wismayer A C 1997 *J. Nucl. Mater.* **244** 51
[9] Johnson P B, Thomson R W and Reader K 1999 *J. Nucl. Mater.* **273** 117
[10] Giri P K, Raineri V, Franzo G and Rimini E 2001 *Phys. Rev.* B **65** 012110
[11] Dhara S *et al* 2005 *Appl. Phys. Lett.* **86** 203119
[12] Chen C C, Yeh C C, Chen C H, Yu M Y, Liu H L, Wu J J, Chen K H, Chen L C, Peng J Y and Chen Y F 2001 *J. Am. Chem. Soc.* **123** 2791
[13] Dhara S, Datta A, Wu C T, Lan Z H, Chen K H, Wang Y L, Chen L C, Hsu C W, Lin H M and Chen C C 2003 *Appl. Phys. Lett.* **82** 451
[14] Dhara S, Datta A, Lan Z H, Chen K H, Wang Y L, Shen C S, Chen L C, Hsu C W, Lin H M and Chen C C 2004 *Appl. Phys. Lett.* **84** 3486
[15] Dhara S, Datta A, Hsu C W, Wu C T, Shen C H, Lan Z H, Chen K H, Chen L C, Wang Y L and Chen C C 2004 *Appl. Phys. Lett.* **84** 5473
[16] Ziegler J F, Biersack J P and Littmark U 1985 *The Stopping and Range of Ions in Solids* (New York: Pergamon) http://www.research.ibm.com/ionbeams/SRIM/
[17] Wang Y L and Shao Z 1991 *Advances in Electronics and Electron Physics* vol 81, ed P W Hawkes (Boston, MA: Academic) p 177
[18] Egerton R F 1996 *Electron Energy-Loss Spectroscopy in the Electron Microscope* vol 431 (New York: Plenum) Appendix C
[19] Keast V J, Scott A J, Kappers M J, Foxon C T and Humphreys C J 2002 *Phys. Rev.* B **66** 125319
[20] Zuger O and Durig U 1992 *Phys. Rev.* B **46** 7319
[21] Neugebauer J and Van de Walle C G 1994 *Diamond, SiC and Nitride Wide-Bandgap Semiconductors* vol 339 ed C H Carter Jr, G Glidenblat, S Nakamura and R J Nemanich (Pittsburgh, PA: MRS Symp. Proc. Materials Research Society) p 687
[22] Neugebauer J and Van de Walle C G 1994 *Phys. Rev.* B **50** 8067
[23] Polian A, Grimsditch M and Grzegory I 1996 *J. Appl. Phys.* **79** 3343